


Particle production by a relativistic semitransparent mirror in (1 + 3)D Minkowski spacetime

Kuan-Nan Lin^{1,2,*}, Chih-En Chou^{1,2,†} and Pisin Chen^{1,2,3,‡}

¹*Leung Center for Cosmology and Particle Astrophysics, National Taiwan University, Taipei 10617, Taiwan, Republic of China*

²*Department of Physics and Center for Theoretical Sciences, National Taiwan University, Taipei 10617, Taiwan, Republic of China*

³*Kavli Institute for Particle Astrophysics and Cosmology, SLAC National Accelerator Laboratory, Stanford University, Stanford, California 94305, USA*

 (Received 9 September 2020; accepted 12 November 2020; published 14 January 2021)

Production of massless, scalar particles by a relativistic, semitransparent, plane mirror in (1 + 3)D Minkowski spacetime based on the Barton-Calogheracos (BC) action is investigated. The corresponding Bogoliubov coefficients are derived for a mirror with arbitrary, relativistic trajectories. We apply our derived formula to two specific trajectories. One is commonly used in the (1 + 1)D literature to mimic gravitational collapse theoretically, and the other is proposed to be realizable experimentally. In addition, we identify the relation between the particle spectrum and the particle production probability, and we demonstrate the equivalence between our approach and the existing approach in the literature, which is restricted to (1 + 1)D. In short, our treatment extends the study to (1 + 3)D spacetime for a relativistic, plane mirror. Lastly, we offer a third approach for finding the particle spectrum using the S-matrix formalism.

DOI: [10.1103/PhysRevD.103.025014](https://doi.org/10.1103/PhysRevD.103.025014)

I. INTRODUCTION

In 1970, Moore demonstrated [1] that quanta of electromagnetic field may be produced from the initial vacuum state if the field is constrained in a one-dimensional cavity and subject to time-dependent Dirichlet boundary conditions in (1 + 1)D Minkowski spacetime. This phenomenon is a manifestation of the interaction between vacuum fluctuations of the quantized field and moving boundaries. A few years later, DeWitt [2] showed that, for a scalar field subject to a single time-dependent Dirichlet boundary condition, i.e., a moving, perfect, point mirror, in (1 + 1)D Minkowski spacetime, the production of particles out of the initial vacuum state is also possible. Soon after, Fulling and Davies studied the energy-momentum tensor [3] and particle spectrum [4] for a perfect, point mirror following prescribed trajectories in (1 + 1)D. The production of particles out of the vacuum due to time-dependent boundary condition(s) is therefore referred to as the: “Moore effect”, “dynamical Casimir effect”, “motion-induced radiation”, or “moving mirror radiation”. For mirrors with a variety of trajectories mimicking different scenarios of black hole radiation, please see Good’s recent works, e.g., [5,6], whereas for various trajectories mimicking

different candidate resolutions to the information loss paradox of black hole evaporation, please see Chen and Yeom [7].

Most works in this subject are studied in (1 + 1)D Minkowski spacetime in which the massless, scalar field and the Klein-Gordon equation are conformal invariant. Conformal invariance allows for exact solutions to the Klein-Gordon equation for a perfect, point mirror in arbitrary motion, i.e., arbitrary time-dependent Dirichlet boundary condition. In addition, when expanding the scalar field in terms of mode functions, the past null infinity \mathcal{I}^- and the future null infinity \mathcal{I}^+ can always serve as the in-region and the out-region, respectively, and thus the concept of particle is well defined in these two regions. Nevertheless, conformal invariance breaks down in higher dimensions and thus the techniques developed for (1 + 1)D no longer apply. Instead, in (1 + 3)D spacetime, the proper in-region and the out-region are, respectively, the remote past ($x_0 \rightarrow -\infty$) and the remote future ($x_0 \rightarrow \infty$). In this case, particle spectra for a nonrelativistic mirror with bounded motions starting and stopping at the same position have been worked out [8–12] based on the perturbative approach proposed by Ford and Vilenkin [13].

Aside from the concept of particles, another physical quantity of common interest is the (local) energy-momentum tensor. This quantity may be easier to obtain than the particle spectrum (if it may be defined) for mirrors with

*r08222037@ntu.edu.tw

†r07222028@ntu.edu.tw

‡pisinchen@phys.ntu.edu.tw

arbitrary trajectories and even in higher dimensional spacetimes since it only requires the knowledge of the in-mode and the in-vacuum. Energy-momentum tensor is, in general, not related to the particle spectrum by a simple mode-summation procedure of adding up the energy carried by each particle, see, e.g., [3–6,13,14], because it also contains the effect of vacuum polarization. Energy-momentum tensor for an infinite-size, plane, Rindler mirror in $(1+3)$ D has been worked out by Candelas and Raine [15] and Candelas and Deutsch [16], while spherical mirrors with shells expanding/contracting with near-uniform acceleration are also studied in, e.g., [17–19].

Limited by technologies, a direct construction of a relativistic mirror in laboratories to test the above studies were not feasible. Therefore, alternative experimental proposals had been conceived and conducted, e.g., the superconducting quantum interference device (SQUID) experiment [20] and references therein. Nevertheless, it is recently proposed by Chen and Mourou [21,22] that the relativistic mirror may be manifested through plasma wakefields.

In actual experiments, such as that proposed in [21,22] that involve physical, relativistic mirrors, one tends to encounter the following situations: (i) the spacetime is $(1+3)$ D Minkowskian, (ii) the mirror is not a perfect reflector, (iii) the mirror is roughly planar, and (iv) the mirror has a finite transverse dimension. Therefore, formulations that incorporate these realistic, less than perfect situations are desirable for the cross-check with future experimental results. In this paper, the approach we adopted, in principle, enables the inclusion of these situations. However, we will only focus on (i), (ii), and (iii) in the present paper and leave (iv) for further discussions in our future work since the aims of the present paper are to lay down the framework that applies to a plane mirror following a general, relativistic trajectory in $(1+3)$ D Minkowski spacetime and to explore new features that do not show up in the standard $(1+1)$ D literature or the studied $(1+3)$ D non-relativistic, plane mirror model.

The first example that we study is the trajectory that is often used to mimic the physics of gravitational collapse of a spherical null shell in $(1+3)$ D curved spacetime in the $(1+1)$ D moving mirror literature. It is fortunate that this trajectory enables an analytic computation and allows us to check whether our $(1+3)$ D results are, in the $\mathbf{k}_\perp = 0$ limit, consistent with the $(1+1)$ D literature that uses different approaches. The corresponding new features that arise in $(1+3)$ D due to the nonvanishing transverse momentum are also readily distinguished from the usual behavior in $(1+1)$ D. Despite this trajectory is not yet realizable in practice, it suffices to meet our aim of the present paper, i.e., to see the emergence of new physical properties when a relativistic, plane mirror is considered. The second example that we study is one of the trajectories proposed in [22] that might be realizable in practice. In this

paper, we study that trajectory under certain assumptions such that analytic computations are possible.

We will begin with the Barton-Calogeracos (BC) action [23]:

$$S_\alpha[\phi] = -\frac{1}{2} \int_{\mathbb{R}} d^4x \partial^\mu \phi(x) \partial_\mu \phi(x) - \frac{\alpha}{2} \int_{\mathbb{R}} d^4x \gamma^{-1}(x_0) \delta(x_3 - q(x_0)) \phi^2(x), \quad (1)$$

where α is a coupling constant with the dimension of length^{-1} , $\gamma(x_0)$ is the usual Lorentz factor, and $q(x_0)$ denotes the mirror's trajectory. In this action, the scalar field $\phi(x)$ interacts quadratically with a Dirac-delta function that simulates the moving mirror. Their interaction is adiabatically switched on and off in the remote past ($x_0 \rightarrow -\infty$) and the remote future ($x_0 \rightarrow \infty$) and thus we will identify them as the in-region and the out-region, respectively. The BC action is applicable to relativistic, partial reflecting mirrors and general spacetime dimensions. The model is equivalent to a jellium sheet of zero width, i.e., a surface of zero thickness with a surface current density generated by the motion of small charge elements with charge density n_s (number of charge elements per unit area) and the coupling constant is identified as $\alpha = 4\pi n_s e^2 / m_e$, where e and m_e are the charge and the mass of the individual entity, respectively [23,24].

Despite the generalizability of the BC action, so far only reductions to $(1+1)$ D or the non-relativistic limit have been studied, e.g., [25–31]. Recently, Fosco, Giraldo and Mazzitelli [32] studied the pair production probability for the BC action in higher dimensional spacetime by using the in-out effective action approach. In this paper, we (i) derive the particle spectrum for a mirror following general, prescribed trajectories by solving the inhomogeneous Klein-Gordon equation for the BC action using the Born approximation and subsequently (ii) identify the relation between the particle spectrum and the particle production probability. In addition, we demonstrate the equivalence of our approach to Nicolaevici's approach [28,29] in the $(1+1)$ D limit.

This paper is organized as follows. In Sec. II, the $(1+3)$ D inhomogeneous Klein-Gordon equation is solved perturbatively. The Bogoliubov transformation between the in-/out-creation and annihilation operators are subsequently derived and the particle spectrum follows straightforwardly. The relation between the particle spectrum and the particle production probability is also identified. In Sec. III, we demonstrate the equivalence between our treatment and the approach adopted in the literature in $(1+1)$ D. In Sec. IV, we apply our $(1+3)$ D formula to two specific trajectories. In Appendix, we offer a third approach for finding the particle spectrum using the S-matrix.

TABLE I. Comparisons between two different perturbative approaches that can be applied to (1+3)D.

	Lin-Chou-Chen	Ford-Vilenkin [13]
Mirror reflectivity	Semi-transparent	Perfect reflector
In-/Out-field	Free field	Static-mirror field
Spacetime dimension	(1+1)D and (1+3)D	(1+1)D and (1+3)D
Coordinate frame	Lab (x_0, x_1, x_2, x_3)	Lab (x_0, x_1, x_2, x_3)
Perturbation in Approach	Coupling constant: α Retarded Green function Advanced Green function	Boundary condition: $q(x_0)/x_3, \dot{q}^2(x_0)$, etc. Retarded Green function Advanced Green function
Valid trajectories	Relativistic	Non-relativistic
Mirror's initial/final location	No restriction	Static at the same location
Beta-coefficient is found by	Fourier transformation	Fourier transformation

In this paper, we use $\hbar = k_B = c = 1$ and the metric signature $(-, +, +, +)$ in (1+3)D. The symbol x refers to $(x_0, \mathbf{x}_\perp, x_3)$, where \mathbf{x}_\perp are the coordinates x_1, x_2 that are transverse to the mirror's motion, $k_\perp \equiv |\mathbf{k}_\perp|$, \mathbb{R} refers to $(-\infty, \infty)$, and \mathbb{R}^+ refers to $(0, \infty)$, etc.

II. PARTICLE PRODUCTION IN (1+3)D

A. Particle spectrum

The equation of motion (EOM) for the BC action is

$$\partial^\mu \partial_\mu \phi(x) = \alpha \gamma^{-1}(x_0) \delta(x_3 - q(x_0)) \phi(x). \quad (2)$$

Due to the linearity of the differential equation, its *solution* [33] can be superposed by

$$\phi(x) = \phi_h(x) + \phi_p(x), \quad (3)$$

where (after second-quantization)

$$\hat{\phi}_h(x) = \int \frac{d^3 k'}{(2\pi)^{3/2} (2|\mathbf{k}'|)^{1/2}} [\hat{a}_{\mathbf{k}'} e^{-i|\mathbf{k}'|x_0 + i\mathbf{k}' \cdot \mathbf{x}} + \text{H.c.}], \quad (4)$$

is the homogeneous solution with its integration range to be determined and

$$\hat{\phi}_p(x) = -\alpha \int_{\mathbb{R}} d^4 x' \gamma^{-1}(x'_0) \delta(x'_3 - q(x'_0)) \hat{\phi}(x') G_R(x, x'), \quad (5)$$

is the particular *solution*; $G_R(x, x')$ is the free field retarded Green function. Applying the Born approximation to the first order in α , we obtain

$$\begin{aligned} \hat{\phi}^{(1)}(x) &= \hat{\phi}_h(x) + \hat{\phi}_p^{(1)}(x) \\ &= \hat{\phi}_h(x) \\ &\quad - \alpha \int_{\mathbb{R}} d^4 x' \gamma^{-1}(x'_0) \delta(x'_3 - q(x'_0)) \hat{\phi}_h(x') G_R(x, x'), \end{aligned} \quad (6)$$

where the homogeneous solution is now

$$\hat{\phi}_h = \int_{\mathbb{D}} \frac{d^3 k'}{(2\pi)^{3/2} (2|\mathbf{k}'|)^{1/2}} [\hat{a}_{\mathbf{k}'} e^{-i|\mathbf{k}'|x_0 + i\mathbf{k}' \cdot \mathbf{x}} + \text{H.c.}]. \quad (7)$$

The domain for the integration over momentum is determined as $\mathbf{k}' \in \mathbb{D}$ by the semitransparent condition: $|\phi_p^{(1)}(x)| \ll |\phi_h(x)|$ due to the first-order approximation made. This constraint would lead to a physical infrared cutoff for the incident free modes. This can be expected directly from physical grounds. Semitransparency of the mirror is just another way of saying the incident modes interact weakly with the mirror, which is comprised of, e.g., electrons. For the interaction to be weak, the incident modes should have wavelengths small enough compared to the spacing between the adjacent electrons so as to pass by the mirror without much scattering. This then imposes the infrared cutoff for $\hat{\phi}^{(1)}(x)$ since the electron density is proportional to the coupling constant α as mentioned in Sec. I. In principle, the perturbation in α can be extended to higher orders since Eq. (3) is an integral equation. Had all the orders been kept, the mirror would then become a perfect reflector for all momenta by taking $\alpha \rightarrow \infty$. Nevertheless, it may be technically impractical to discuss the high reflection case by using the perturbative approach. As a side remark, comparisons between our and Ford-Vilenkin's perturbative approach are summarized in Table I and comparisons between our and Nicolaevici's, Haro-Elizalde's approaches, which are exact in α , are summarized in Table II.

The counterpart of $\phi^{(1)}(x)$ using the free field advanced Green function, $G_A(x, x')$, is similarly obtained:

$$\begin{aligned} \hat{\phi}^{(1)}(x) &= \hat{\phi}_h(x) \\ &\quad - \alpha \int_{\mathbb{R}} d^4 x' \gamma^{-1}(x'_0) \delta(x'_3 - q(x'_0)) \hat{\phi}_h(x') G_A(x, x'). \end{aligned} \quad (8)$$

Using the retarded Green function, we are in fact assuming the vacuum state defined by $\hat{a}_{\mathbf{k}}^{\text{in}}|0, \text{in}\rangle = 0$. In addition, since we are considering the first-order field, we

TABLE II. Comparisons between different approaches for a relativistic, partially reflecting mirror.

	Lin-Chou-Chen	Nicolaevici [28,29]	Haro-Elizalde [25]
Action	Barton-Calogeracos action	Barton-Calogeracos action	Barton-Calogeracos action
Spacetime dimension	(1 + 1)D and (1 + 3)D	(1 + 1)D	(1 + 1)D
Coordinate frame	Lab (x_0, x_1, x_2, x_3)	Lab (u, v)	Lab (u, v) Comoving (\bar{u}, \bar{v})
Perturbation or exact	Perturbation in α	Exact in α	Exact in α
Approach	Retarded Green function Advanced Green function	Differential equation for reflection coefficient	Conformal transformation of S-matrix elements
Valid trajectories	Relativistic	Relativistic	Relativistic
Mirror's initial/final location	No restriction	No restriction	No restriction
Beta-coefficient is found by	Fourier transformation	Klein-Gordon inner product	Klein-Gordon inner product

may identify the homogeneous part of (8) as the out-field while the remaining $\hat{\phi}_h$ in (6) and (8) as the in-field.

To obtain the knowledge of creation and annihilation operators, we Fourier transform $\hat{\phi}^{(1)}(x)$ by

$$\int_{\mathbb{R}} dx_0 d^2 x_{\perp} \int_0^{\infty} dx_3 \hat{\phi}^{(1)}(x) e^{i\omega x_0 - i\mathbf{k}\cdot\mathbf{x}}, \quad (9)$$

and use the Green functions of the following form

$$G_{R/A}(x, x') = \int_{\mathbb{R}} \frac{d\omega}{2\pi} \frac{e^{-i\omega(x_0 - x'_0) \pm i\omega|\mathbf{x} - \mathbf{x}'|}}{4\pi|\mathbf{x} - \mathbf{x}'|}, \quad (10)$$

where the Weyl identity for $\omega \in \mathbb{R}^+$

$$\frac{e^{i\omega|\mathbf{x} - \mathbf{x}'|}}{4\pi|\mathbf{x} - \mathbf{x}'|} = \frac{i}{8\pi^2} \int_{\mathbb{R}} d^2 k_{\perp} \frac{e^{i\mathbf{k}_{\perp} \cdot (\mathbf{x}_{\perp} - \mathbf{x}'_{\perp}) + i(\omega^2 - k_{\perp}^2)^{1/2} |x_3 - x'_3|}}{(\omega^2 - k_{\perp}^2)^{1/2}}, \quad (11)$$

is to be used in the calculation. To proceed with computational ease, we temporary assume $q(x'_0) \leq 0 \quad \forall \quad x'_0$ since x_3 is already positive in (9). Finally, by equating the Fourier transform of (6) and (8) and subsequently choosing $\omega > 0$, $(\omega^2 - k_{\perp}^2)^{1/2} > 0$, and $k_3 = (\omega^2 - k_{\perp}^2)^{1/2} > 0$ after lengthy calculations, we obtain the Bogoliubov transformation on the mirror's right as

$$\begin{aligned} \hat{a}_{\mathbf{k}_{\perp} k_3}^{\text{out}} &\approx \hat{a}_{\mathbf{k}_{\perp} k_3}^{\text{in}} + \frac{\alpha}{4\pi i} \frac{1}{|\mathbf{k}|^{1/2}} \int_{\mathbb{R}} dx'_0 \int_{\mathbb{D}} dk'_3 \frac{\gamma^{-1}(x'_0)}{(k_{\perp}^2 + k_3^2)^{1/4}} \\ &\times \left[\hat{a}_{\mathbf{k}_{\perp} k'_3}^{\text{in}} e^{-i(\sqrt{k_{\perp}^2 + k_3^2} - |\mathbf{k}|)x'_0 + i(k'_3 - k_3)q(x'_0)} + \hat{a}_{-\mathbf{k}_{\perp} k'_3}^{\text{in}\dagger} e^{i(\sqrt{k_{\perp}^2 + k_3^2} + |\mathbf{k}|)x'_0 - i(k'_3 + k_3)q(x'_0)} \right], \end{aligned} \quad (12)$$

where

$$\beta_{\mathbf{k}\mathbf{k}'} \approx \frac{\alpha}{4\pi i} \frac{1}{|\mathbf{k}|^{1/2}} \int_{\mathbb{R}} dx'_0 \frac{\gamma^{-1}(x'_0)}{(k_{\perp}^2 + k_3^2)^{1/4}} e^{i(\sqrt{k_{\perp}^2 + k_3^2} + |\mathbf{k}|)x'_0 - i(k'_3 + k_3)q(x'_0)}, \quad (13)$$

is our desired beta-coefficient that is relevant to particles emitted to the mirror's right. Similarly, choosing $\omega > 0$, $(\omega^2 - k_{\perp}^2)^{1/2} > 0$ and $k_3 = -(\omega^2 - k_{\perp}^2)^{1/2} < 0$, one obtains the same expression of Bogoliubov transformation as above but with k_3 now being negative and the corresponding beta-coefficient is relevant to particles emitted to the mirror's left.

The number of particles with $\mathbf{k} \in \mathbb{D}$ per mode in the out-region is thus

$$\begin{aligned} \frac{dN}{d^2 k_{\perp} dk_3} &= \langle 0, \text{in} | \hat{a}_{\mathbf{k}_{\perp} k_3}^{\text{out}\dagger} \hat{a}_{\mathbf{k}_{\perp} k_3}^{\text{out}} | 0, \text{in} \rangle \\ &= \frac{A}{4\pi^2} \int_{\mathbb{D}} dk'_3 |\beta_{\mathbf{k}\mathbf{k}'}|^2 \\ &\approx \frac{A\alpha^2}{64\pi^4 |\mathbf{k}|} \int_{\mathbb{D}} dk'_3 \frac{1}{\sqrt{k_{\perp}^2 + k_3^2}} \left| \int_{\mathbb{R}} dx'_0 \gamma^{-1}(x'_0) e^{i(|\mathbf{k}| + \sqrt{k_{\perp}^2 + k_3^2})x'_0 - i(k_3 + k'_3)q(x'_0)} \right|^2, \end{aligned} \quad (14)$$

where A is the area of the infinite-size, plane mirror. The beta-coefficient and particle spectrum in (1 + 1)D follow directly from (13) and (14) by letting $\mathbf{k}_{\perp} = 0$.

B. Particle production probability

The vacuum persistence amplitude \mathcal{Z}_α corresponding to the BC action is defined as

$$\mathcal{Z}_\alpha = e^{iW_\alpha} = \int \mathcal{D}\phi e^{iS_\alpha[\phi]}, \quad (15)$$

where W_α is the effective action. By decomposing W_α as $W_\alpha = W_0 + W_I$, where W_0 is the effective action in the absence of interaction, i.e., free field effective action, the interaction effective action W_I can be written as

$$e^{iW_I} = \langle 0 | \mathcal{T} e^{-\frac{i\alpha}{2} \int_{\mathbb{R}} d^4x \gamma^{-1}(x_0) \delta(x_3 - q(x_0)) \hat{\phi}^2(x)} | 0 \rangle, \quad (16)$$

where \mathcal{T} is the time-ordering operator, $\hat{\phi}$ is a free scalar field operator, and $|0\rangle$ is the free field vacuum state. By expanding to the second order in α and using Wick's theorem, we obtain

$$\begin{aligned} e^{iW_I} &\approx 1 + \frac{\alpha}{2} \int_{\mathbb{R}} d^4x \gamma^{-1}(x_0) \delta(x_3 - q(x_0)) G_F(x, x) \\ &+ \frac{\alpha^2}{8} \left[\int_{\mathbb{R}} d^4x \gamma^{-1}(x_0) \delta(x_3 - q(x_0)) G_F(x, x) \right]^2 \\ &+ \frac{\alpha^2}{4} \int_{\mathbb{R}} d^4x d^4x' \gamma^{-1}(x_0) \delta(x_3 - q(x_0)) \\ &\times \gamma^{-1}(x'_0) \delta(x'_3 - q(x'_0)) G_F^2(x, x'), \end{aligned} \quad (17)$$

where $G_F(x, x')$ is the free field Feynman propagator. The constant factors in the denominator of each term are the symmetry factors for the corresponding processes. For example, the symmetry factor 2 for the $\mathcal{O}(\alpha)$ process comes from the propagator starting and ending on the same spacetime point (vertex); the factor $4 = 2 \times 2^1 \times 1!$ for the last term originates, respectively, from (i) two propagators connecting x and x' , (ii) $2^{2/2} = 2^1$ ways of choosing $2/2 = 1$ vertex among the 2 vertices as an in vertex, and (iii) $1!$ way to pair the in vertex with the remaining (out) vertex. W_I is approximately

$$\begin{aligned} iW_I &\approx \frac{\alpha}{2} G_F(0) A \int_{\mathbb{R}} d\tau + \frac{\alpha^2}{4} \int_{\mathbb{R}} d^4x d^4x' \gamma^{-1}(x_0) \\ &\times \delta(x_3 - q(x_0)) \gamma^{-1}(x'_0) \delta(x'_3 - q(x'_0)) G_F^2(x, x'), \end{aligned} \quad (18)$$

where we have used $\ln(1+x) \approx x - x^2/2$ and τ is the mirror's proper time. The above equation has also been derived in [32]. However, in our following treatment, we use the following expression for the Feynman propagator:

$$\begin{aligned} G_F(x, x') &= -i\Theta(\Delta x_0) \int_{\mathbb{R}} \frac{d^3k}{(2\pi)^3} \frac{e^{-i|\mathbf{k}|\Delta x_0 + i\mathbf{k}\cdot\Delta\mathbf{x}}}{2|\mathbf{k}|} \\ &- i\Theta(-\Delta x_0) \int_{\mathbb{R}} \frac{d^3k}{(2\pi)^3} \frac{e^{i|\mathbf{k}|\Delta x_0 + i\mathbf{k}\cdot\Delta\mathbf{x}}}{2|\mathbf{k}|}, \end{aligned} \quad (19)$$

where Θ is the Heaviside step function, $\Delta x_0 = x_0 - x'_0$, $\Delta\mathbf{x} = \mathbf{x} - \mathbf{x}'$, and replace $\Theta(-\Delta x_0)$ by $1 - \Theta(\Delta x_0)$ instead

of using Feynman parametrization as [32] did, we then obtain the probability of particle production as

$$\begin{aligned} \mathcal{P} &\approx 2\text{Im}W \approx \frac{1}{2} \int_{\mathbb{D}} d^3k \frac{A\alpha^2}{64\pi^4 |\mathbf{k}|} \int_{\mathbb{D}} dk'_3 \frac{1}{\sqrt{k_\perp^2 + k_3'^2}} \\ &\times \left| \int_{\mathbb{R}} dx'_0 \gamma^{-1}(x'_0) e^{i(|\mathbf{k}| + \sqrt{k_\perp^2 + k_3'^2})x'_0 - i(k_3 + k'_3)q(x'_0)} \right|^2, \end{aligned} \quad (20)$$

where the factor of $1/2$ on the right-hand side is the product of $2 \times 1/4$. Note that the domains for the momenta are \mathbb{D} since we are only considering the case of a semi-transparent mirror, i.e., second order in α for the probability. Finally, by comparing (20) with (14), we observe that the probability of particle production is related to the particle spectrum by

$$\mathcal{P} \approx 2\text{Im}W \approx \frac{1}{2} \int_{\mathbb{D}} d^3k \frac{dN}{d^2k_\perp dk_3}. \quad (21)$$

III. EQUIVALENCE OF DIFFERENT APPROACHES IN (1+1)D

A. Our approach

From (6), which applies in (1+3)D, we can deduce the in-mode in (1+1)D straightforwardly by

$$\begin{aligned} u^{(1)}(t, x) &\approx u_h(t, x) - \alpha \int_{\mathbb{R}} dt'_m dx' \gamma^{-1}(t'_m) \\ &\times \delta(x' - z_m(t'_m)) u_h(t'_m, x') G_R(t, x; t'_m, x'), \end{aligned} \quad (22)$$

where

$$\begin{aligned} G_R(t, x; t'_m, x') &= \frac{1}{2} \Theta(t - t'_m - |x - x'|) \\ &= \frac{1}{2} \int_{-\infty}^t dt'' \delta(t'' - t'_m - |x - x'|), \end{aligned} \quad (23)$$

is the (1+1)D retarded Green function, and we have changed the notations for the mirror's trajectory by $q(x'_0) \rightarrow z_m(t'_m)$, the observation points by $x_0 \rightarrow t$, $x_3 \rightarrow x$, and the dummy variables by $x'_0 \rightarrow t'_m$, $x'_3 \rightarrow x'$ for a clear correspondence with the typical (1+1)D literature.

For $u_h(t, x) = e^{-i\omega t - i\omega x}$ and on the mirror's right, i.e., $x - z_m(t'_m) > 0$, the inhomogeneous part of (22) can be evaluated as

$$\begin{aligned} &-\frac{\alpha}{2} \int_{-\infty}^t dt'' \int_{\mathbb{R}} dt'_m \gamma^{-1}(t'_m) e^{-i\omega t'_m - i\omega z_m(t'_m)} \\ &\times \delta(t'' - t'_m - x + z_m(t'_m)) \\ &= -\frac{\alpha}{2} \int_{-\infty}^t dt'' \int \frac{dR(t'_m)}{1 - \dot{z}_m(t'_m)} \gamma^{-1}(t'_m) \\ &\times e^{-i\omega t'_m - i\omega z_m(t'_m)} \delta(t'' - x - R(t'_m)) \\ &= -\frac{\alpha}{2} \int_{-\infty}^{t_m(u)} dt'_m \gamma^{-1}(t'_m) e^{-i\omega t'_m - i\omega z_m(t'_m)}, \end{aligned} \quad (24)$$

where $R(t'_m) = t'_m - z_m(t'_m)$ in the first equality and $R(t_m) = t - x$ in the last equality. Notice that $R(t_m) = t - x$ recovers the standard condition for an out-going massless particle in the null coordinates $u = t - x$, and hence we denote t_m by $t_m(u)$. On the mirror's left, i.e., $x - z_m(t'_m) < 0$, we have

$$\begin{aligned} & -\frac{\alpha}{2} \int_{-\infty}^{t_m(v)} dt'_m \gamma^{-1}(t'_m) e^{-i\omega t'_m - i\omega z_m(t'_m)} \\ &= -\frac{\alpha}{2} \int_{-\infty}^{t_m(u)} dt'_m \gamma^{-1}(t'_m) e^{i\omega[t_m + z_m(t_m) - t'_m - z_m(t'_m)]} e^{-i\omega t - i\omega x}, \end{aligned} \quad (25)$$

instead, where $t_m(v)$ is determined by $t_m + z_m(t_m) = t + x$, which again recovers the standard condition $v = t + x$ for an in-coming massless particle.

For the out-mode, we use the advanced Green function

$$\begin{aligned} G_A(t, x; t'_m, x') &= \frac{1}{2} \Theta(t'_m - t - |x - x'|) \\ &= -\frac{1}{2} \int_{\infty}^t dt'' \delta(t'_m - t'' - |x - x'|), \end{aligned} \quad (26)$$

in (22) instead. Following the same procedure as above, we find, for $u_h(t, x) = e^{-i\omega t + i\omega x}$ and on the mirror's right, i.e., $x - z_m(t'_m) > 0$, the inhomogeneous part as

$$-\frac{\alpha}{2} \int_{t_m(v)}^{\infty} dt'_m \gamma^{-1}(t'_m) e^{-i\omega t'_m + i\omega z_m(t'_m)}. \quad (27)$$

The other situations, e.g., $u_h(t, x) = e^{-i\omega t - i\omega x}$ and on the mirror's left, may be straightforwardly found by using the same procedure and thus we shall not repeat it here.

B. Nicolaevici's approach

The in-mode given by Nicolaevici [28,29] is, e.g.,

$$V^R = e^{-i\omega v} - R^R(u) e^{-i\omega p(u)}, \quad V^L = T^L(v) e^{-i\omega v}, \quad (28)$$

where the superscripts R/L refer to the mirror's right/left, (u, v) are the $(1+1)$ D null coordinates, and the ray-tracing function is

$$p(u) = 2z_m(u) + u, \quad (29)$$

and the reflection and transmission coefficients are [34]

$$\begin{aligned} R^R(u) &= \frac{\alpha}{2} \int_{-\infty}^{\tau} dt' e^{-\frac{\alpha}{2}(\tau - t') + i\omega[v(\tau) - v(t')]}, \\ T^L(v) &= 1 - R^R(u), \end{aligned} \quad (30)$$

where τ is the mirror's proper time and $v(\tau) = t_m(u) + z_m(t_m) = p(u)$. In the first-order approximation, which corresponds to the semitransparent limit [35], the reflection coefficient becomes

$$R^R(u) \approx \frac{\alpha}{2} \int_{-\infty}^{\tau} dt' e^{i\omega[v(\tau) - v(t')]}. \quad (31)$$

Therefore, we have

$$\begin{aligned} -R^R(u) e^{-i\omega p(u)} &\approx -\frac{\alpha}{2} \int_{-\infty}^{\tau} dt' e^{-i\omega t'_m - i\omega z_m(t'_m)} \\ &= -\frac{\alpha}{2} \int_{-\infty}^{t_m(u)} dt'_m \gamma^{-1}(t'_m) e^{-i\omega t'_m - i\omega z_m(t'_m)}, \end{aligned} \quad (32)$$

which recovers our result (24).

The out-mode is given by [28,29]

$$U^R = e^{-i\omega u} - R^R(v) e^{-i\omega f(v)}, \quad U^L = T^L(u) e^{-i\omega u}, \quad (33)$$

where the ray-tracing function is

$$f(v) = -2z_m(v) + v, \quad (34)$$

and the reflection and transmission coefficients are

$$\begin{aligned} R^R(v) &= \frac{\alpha}{2} \int_{\tau}^{\infty} dt' e^{\frac{\alpha}{2}(\tau - t') + i\omega[u(\tau) - u(t')]}, \\ T^L(u) &= 1 - R^R(v), \end{aligned} \quad (35)$$

where $u(\tau) = t_m(v) - z_m(t_m) = f(v)$. In the first-order limit, we obtain

$$-R^R(v) e^{-i\omega f(v)} \approx -\frac{\alpha}{2} \int_{t_m(v)}^{\infty} dt'_m \gamma^{-1}(t'_m) e^{-i\omega t'_m + i\omega z_m(t'_m)}, \quad (36)$$

which is identical to our (27).

The beta-coefficients on the mirror's right using Nicolaevici's modes are

$$\begin{aligned} \beta_{\omega\omega'}^{\text{ref}} &= -\langle U^{\text{out}*}(\omega > 0), V^{\text{in}}(\omega' > 0) \rangle_{\text{KG}} \\ &\stackrel{\text{IBP}}{=} -\left[\frac{\omega}{2\pi\sqrt{\omega\omega'}} \int_{-\infty}^{\infty} du R^R(u) e^{-i\omega' p(u)} e^{-i\omega u} \right]^* \\ &\stackrel{\text{IBP}}{\approx} \frac{\alpha}{4\pi i\sqrt{\omega\omega'}} \int_{-\infty}^{\infty} du \frac{\gamma^{-1}(t_m)}{1 - \dot{z}_m(t_m)} e^{i(\omega + \omega')t_m - i(\omega - \omega')z_m(t_m)} \\ &= \frac{\alpha}{4\pi i\sqrt{\omega\omega'}} \int_{-\infty}^{\infty} dt_m \gamma^{-1}(t_m) e^{i(\omega + \omega')t_m - i(\omega - \omega')z_m(t_m)}, \end{aligned} \quad (37)$$

where the superscript “*ref*” refers to the beta-coefficient contributed by the reflected modes, “*IBP*” refers to integration by parts, $du = (1 - \dot{z}_m(t_m)) dt_m$, and $\langle \cdot \cdot \rangle_{\text{KG}}$ is the Klein-Gordon inner product defined by

$$\langle A, B \rangle_{KG} = -i \int_{\mathbb{R}} du [A(u, v) \overleftrightarrow{\partial}_u B^*(u, v)]_{v \rightarrow \infty}. \quad (38)$$

For the beta-coefficient contributed by the transmitted modes, the other set of in-mode is required, see [28,29]. Since the discussion is similar, we simply list the result we obtained:

$$\beta_{\omega\omega'}^{\text{tran}} \approx \frac{\alpha}{4\pi i} \frac{1}{\sqrt{\omega\omega'}} \int_{-\infty}^{\infty} dt_m \gamma^{-1}(t_m) e^{i(\omega+\omega')t_m - i(\omega+\omega')z_m(t_m)}. \quad (39)$$

The above coefficients agree with the (1+1)D limit of (13) for $k'_3 < 0$ and $k'_3 > 0$, respectively.

We have now completed the demonstration of the equivalence between our approach and the literature's since we are able to obtain identical expressions for the mode functions and the beta-coefficients by further manipulating the standard expressions by integration by parts and a change of variable. Notice that the approach adopted and the expressions given in the standard literature are restricted to (1+1)D since those analyses are based on the null coordinates. Nevertheless, our treatment and expressions extend the discussion to higher dimensions.

IV. EXAMPLES

A. Trajectory 1

We now apply our (1+3)D formula, Eq. (13), to the trajectory that is used to mimic the physics of gravitational collapse of a spherical null shell in (1+3)D curved spacetime in the (1+1)D moving mirror literature [25–28]. By comparing with the (1+1)D literature, we identify properties that are exclusive to the plane mirror model in higher, (1+3)-dimensional spacetime, whereas the conventional (1+1)D results are reproduced by taking the limit: $\mathbf{k}_\perp = 0$. In addition to the trajectory's connection with gravitational collapse, this trajectory is also one of the few trajectories that allows analytic studies and thus it helps to develop intuitions for particle production by a relativistic, plane mirror in (1+3)D flat spacetime.

In this section, the trajectory of interest is

$$z_m(t_m) = \begin{cases} 0, & -\infty < t_m \leq 0 \\ -t_m + \frac{1}{\kappa} - \frac{W[e^{1-2\kappa t_m}]}{\kappa}, & 0 \leq t_m < \infty, \end{cases} \quad (40)$$

where $W(x)$ is the product logarithm and κ is a parameter that can be identified as a black hole's surface gravity in the (1+1)D literature. Note that, in the following discussion, we will change the notations in (13) by $q \rightarrow z_m$ and $x'_0 \rightarrow t_m$. This mirror is initially static and it begins to execute Carlitz-Willey(CW)-like acceleration after $t_m = 0$ toward timelike infinity. The following list the results for quantities in the acceleration phase that will appear in our later computation.

$$\begin{aligned} \frac{dz_m}{dt_m} &= -\frac{1 - W[e^{1-2\kappa t_m}]}{1 + W[e^{1-2\kappa t_m}]}, \\ \gamma^{-1}(t_m) &= \frac{2\sqrt{W[e^{1-2\kappa t_m}]}}{1 + W[e^{1-2\kappa t_m}]}. \end{aligned} \quad (41)$$

On the mirror's right, the beta-coefficient due to the reflected mode may be evaluated by

$$\begin{aligned} \beta_{\mathbf{k}\mathbf{k}'}^{\text{ref}}(k'_3 > 0) &\approx \frac{\alpha}{4\pi i} \frac{1}{\sqrt{|\mathbf{k}||\mathbf{k}'|}} \int_{-\infty}^{\infty} dt_m \gamma^{-1}(t_m) e^{i(|\mathbf{k}|+|\mathbf{k}'|)t_m - i(k_3-k'_3)z_m(t_m)} \\ &= -\frac{\alpha}{4\pi\sqrt{|\mathbf{k}||\mathbf{k}'|}} \left[\frac{1}{|\mathbf{k}|+|\mathbf{k}'|} \right] \\ &\quad + \frac{\alpha}{4\pi i} \frac{1}{\sqrt{|\mathbf{k}||\mathbf{k}'|}} \int_0^{\infty} dt_m \gamma^{-1}(t_m) e^{i(|\mathbf{k}|+|\mathbf{k}'|)t_m - i(k_3-k'_3)z_m(t_m)}. \end{aligned}$$

By making the change of variable:

$$\begin{aligned} d\zeta &= \frac{2W[e^{1-2\kappa t_m}]}{1 + W[e^{1-2\kappa t_m}]} dt_m \\ \zeta &= \frac{1}{\kappa} - \frac{W[e^{1-2\kappa t_m}]}{\kappa}, \quad t_m = \frac{\zeta}{2} - \frac{1}{2\kappa} \ln(1 - \kappa\zeta), \end{aligned} \quad (42)$$

we obtain

$$\begin{aligned} \beta_{\mathbf{k}\mathbf{k}'}^{\text{ref}}(k'_3 > 0) &\approx -\frac{\alpha}{4\pi\sqrt{|\mathbf{k}||\mathbf{k}'|}} \left[\frac{1}{|\mathbf{k}|+|\mathbf{k}'|} \right] + \frac{\alpha}{4\pi i} \frac{1}{\sqrt{|\mathbf{k}||\mathbf{k}'|}} \int_0^{\frac{1}{\kappa}} d\zeta (1 - \kappa\zeta)^{-\frac{1}{2} - \frac{i}{2\kappa}(|\mathbf{k}|+k_3+|\mathbf{k}'|-k'_3)} e^{\frac{i}{2}(|\mathbf{k}|-k_3+|\mathbf{k}'|+k'_3)\zeta} \\ &= -\frac{\alpha}{4\pi\sqrt{|\mathbf{k}||\mathbf{k}'|}} \left[\frac{1}{|\mathbf{k}|+|\mathbf{k}'|} \right] + \frac{\alpha}{4\pi i \kappa} \frac{e^{\frac{i}{2\kappa}(|\mathbf{k}|-k_3+|\mathbf{k}'|+k'_3)}}{\sqrt{|\mathbf{k}||\mathbf{k}'|}} \int_0^1 dz z^{-\frac{1}{2} - \frac{i}{2\kappa}(|\mathbf{k}|+k_3+|\mathbf{k}'|-k'_3)} e^{-\frac{i}{2\kappa}(|\mathbf{k}|-k_3+|\mathbf{k}'|+k'_3)z}, \end{aligned}$$

where $z = 1 - \kappa\zeta$. Next, performing a contour integration in the lower complex plane of z and deforming the contour away from the pole $z = 0$ (this small arc gives no contribution), we obtain

$$\beta_{\mathbf{k}\mathbf{k}'}^{\text{ref}}(k'_3 > 0) \approx -\frac{\alpha}{4\pi\sqrt{|\mathbf{k}||\mathbf{k}'|}} \left[\frac{1}{|\mathbf{k}| + |\mathbf{k}'|} \right] - \frac{\alpha}{4\pi\kappa\sqrt{|\mathbf{k}||\mathbf{k}'|}} \left[e^{\frac{i}{2\kappa}(|\mathbf{k}|-k_3+|\mathbf{k}'|+k'_3)} e^{\frac{i\pi}{4}} e^{-\frac{\pi}{4\kappa}(|\mathbf{k}|+k_3+|\mathbf{k}'|-k'_3)} \right. \\ \left. \times \underbrace{\int_0^\infty ds s^{-\frac{1}{2}-\frac{i}{2\kappa}(|\mathbf{k}|+k_3+|\mathbf{k}'|-k'_3)} e^{-\frac{(|\mathbf{k}|-k_3+|\mathbf{k}'|+k'_3)s}{2\kappa}}}_{z=-is} - \underbrace{\int_0^\infty ds (1-is)^{-\frac{1}{2}-\frac{i}{2\kappa}(|\mathbf{k}|+k_3+|\mathbf{k}'|-k'_3)} e^{-\frac{(|\mathbf{k}|-k_3+|\mathbf{k}'|+k'_3)s}{2\kappa}}}_{z=1-is} \right].$$

The integrals can be evaluated in terms of Gamma and upper incomplete Gamma functions and the result is

$$\beta_{\mathbf{k}\mathbf{k}'}^{\text{ref}}(k'_3 > 0) \approx -\frac{\alpha}{4\pi\sqrt{\omega\omega'}} \left[\frac{1}{\omega + \omega'} \right] - \frac{\alpha e^{\frac{i\omega'_-}{2\kappa}} e^{\frac{i\pi}{4}} e^{-\frac{\pi\omega'_-}{4\kappa}}}{4\pi\kappa\sqrt{\omega\omega'}} \left[\frac{2\kappa}{\omega'_-} \right]^{\frac{1}{2}-\frac{i\omega'_-}{2\kappa}} \left\{ \Gamma \left[\frac{1}{2} - \frac{i\omega'_+}{2\kappa} \right] - \Gamma \left[\frac{1}{2} - \frac{i\omega'_+}{2\kappa}, \frac{i\omega'_-}{2\kappa} \right] \right\}, \quad (43)$$

where we have defined $\omega'_+ = |\mathbf{k}| + k_3 + |\mathbf{k}'| - k'_3$, $\omega'_- = |\mathbf{k}| - k_3 + |\mathbf{k}'| + k'_3$, and $\omega = |\mathbf{k}| = (\mathbf{k}_\perp^2 + k_3^2)^{1/2}$, $\omega' = |\mathbf{k}'| = (\mathbf{k}'_\perp^2 + k'_3^2)^{1/2}$ for brevity. Following similar procedures, we obtain the beta-coefficient due to the transmitted modes as

$$\beta_{\mathbf{k}\mathbf{k}'}^{\text{tran}}(k'_3 > 0) \approx -\frac{\alpha}{4\pi\sqrt{\omega\omega'}} \left[\frac{1}{\omega + \omega'} \right] - \frac{\alpha e^{\frac{i\omega'_-}{2\kappa}} e^{\frac{i\pi}{4}} e^{-\frac{\pi\omega'_-}{4\kappa}}}{4\pi\kappa\sqrt{\omega\omega'}} \left[\frac{2\kappa}{\omega'_-} \right]^{\frac{1}{2}-\frac{i\omega'_-}{2\kappa}} \left\{ \Gamma \left[\frac{1}{2} - \frac{i\omega'_+}{2\kappa} \right] - \Gamma \left[\frac{1}{2} - \frac{i\omega'_+}{2\kappa}, \frac{i\omega'_-}{2\kappa} \right] \right\}, \quad (44)$$

where $\omega'_+ = |\mathbf{k}| + k_3 + |\mathbf{k}'| - k'_3$, $\omega'_- = |\mathbf{k}| - k_3 + |\mathbf{k}'| - k'_3$.

Equations (43) and (44) apply in (1+3)D for $\mathbf{k}, \mathbf{k}' \in \mathbb{D}$ satisfying the semitransparent condition. However, we will take this physical infrared cutoffs for k_3, k'_3 as $k_c \sim \alpha$ in this paper for simplicity.

1. Case 1: $\mathbf{k}_\perp = 0$ ((1+1)D limit)

Perpendicular modes are effectively (1+1)D.

Letting $\mathbf{k}_\perp = 0$ in (43) and (44) give

$$\beta_{\omega\omega'}^{\text{ref}} \approx -\frac{\alpha}{4\pi\sqrt{\omega\omega'}} \left[\frac{1}{\omega + \omega'} \right] - \frac{\alpha e^{\frac{i\omega'_-}{\kappa}} e^{\frac{i\pi}{4}}}{4\pi\kappa\sqrt{\omega\omega'}} \left[\frac{\kappa}{\omega'} \right]^{\frac{1}{2}-\frac{i\omega'_-}{\kappa}} e^{-\frac{\pi\omega'_-}{2\kappa}} \\ \times \left\{ \Gamma \left[\frac{1}{2} - \frac{i\omega}{\kappa} \right] - \Gamma \left[\frac{1}{2} - \frac{i\omega}{\kappa}, \frac{i\omega'}{\kappa} \right] \right\}, \quad (45)$$

and

$$\beta_{\omega\omega'}^{\text{tran}} \approx -\frac{\alpha}{4\pi\sqrt{\omega\omega'}} \left[\frac{1}{\omega + \omega'} \right] \\ + \frac{\alpha}{4\pi i \sqrt{\omega\omega'}} \left[\frac{2}{\kappa - 2i(\omega + \omega')} \right]. \quad (46)$$

In the high frequency regime: $\omega' \gg \kappa$ for $\beta_{\omega\omega'}^{\text{ref}}$, using the asymptotic behavior for the upper incomplete Gamma function, i.e., $\Gamma(s, n) \approx n^{s-1} e^{-n}$ for $n \rightarrow \infty$, the third term exactly cancels out the first term in $\beta_{\omega\omega'}^{\text{ref}}$ by further assuming $\omega' \gg \omega$ (late time). The remaining contribution to $\beta_{\omega\omega'}^{\text{ref}}$ is the second term and it gives

$$|\beta_{\omega\omega'}^{\text{ref}}|^2 \approx \frac{\alpha^2}{8\pi\kappa\omega\omega'^2} \left[\frac{1}{e^{2\pi\omega/\kappa} + 1} \right], \quad (47)$$

which reproduces the spectrum in Refs. [25–28]. At this point, $\omega > k_c$ while $\omega' > k_c$, $\omega' \gg \kappa$, and $\omega' \gg \omega$. On the other hand, all the terms in (46) combine to give

$$|\beta_{\omega\omega'}^{\text{tran}}|^2 \approx \frac{\alpha^2 \kappa^2}{16\pi^2 \omega\omega'} \frac{1}{(\omega + \omega')^2 [\kappa^2 + 4(\omega + \omega')^2]}. \quad (48)$$

2. Case 2: $\omega_- \ll \kappa$

For $\omega'_- \ll \kappa$, the first term in $\beta_{\mathbf{k}\mathbf{k}'}^{\text{ref}}$ dominates:

$$|\beta_{\mathbf{k}\mathbf{k}'}^{\text{ref}}(k'_3 > 0)|^2 \approx \frac{\alpha^2}{16\pi^2 \omega\omega'} \frac{1}{(\omega + \omega')^2}. \quad (49)$$

For $0 < \omega'_- \ll \kappa$, the first term in $\beta_{\mathbf{k}\mathbf{k}'}^{\text{tran}}$ dominates:

$$|\beta_{\mathbf{k}\mathbf{k}'}^{\text{tran}}(k'_3 > 0)|^2 \approx \frac{\alpha^2}{16\pi^2 \omega\omega'} \frac{1}{(\omega + \omega')^2}. \quad (50)$$

3. Case 3: $\omega' \gg \omega$ (late time) $\wedge \omega' \gg \kappa$

In this case, only the second term in $\beta_{\mathbf{k}\mathbf{k}'}^{\text{ref}}$ survives:

$$|\beta_{\mathbf{k}\mathbf{k}'}^{\text{ref}}(k'_3 > 0)|^2 \approx \frac{\alpha^2}{8\pi\kappa\omega k_3^2} \left[1 - \frac{3(\omega \sin \theta)^2}{4k_3^2} \right] \left[\frac{1}{e^{\omega/T_{\text{eff}}(\theta)} + 1} \right], \quad (51)$$

where $T_{\text{eff}}(\theta) = \kappa/[(1 + \cos \theta)\pi]$ is identified as an effective temperature. At this point, the conditions required are: $k_3 > k_c$, $k'_3 > k_c$, $\omega' \sim k'_3 \gg \omega$, and $\omega' \sim k'_3 \gg \kappa$.

On the other hand, to expand the incomplete Gamma function for $\omega'_- \gg \kappa$ in $\beta_{\mathbf{k}\mathbf{k}'}^{\text{tran}}$, the additional conditions: $\theta \neq 0$ and $\omega \gg \kappa$ are required. However, in such a case, the third term no longer cancels with the first term in $\beta_{\mathbf{k}\mathbf{k}'}^{\text{tran}}$

but only indicates the latter is negligible compared to the former. Nevertheless, since $\omega' \gg \kappa$, the third term is negligible compared to the second term. Therefore, at the end of the day, the second term in $\beta_{\mathbf{k}\mathbf{k}'}^{\text{tran}}$ dominates and gives

$$|\beta_{\mathbf{k}\mathbf{k}'}^{\text{tran}}(k'_3 > 0)|^2 \approx \frac{\alpha^2}{4\pi\kappa\omega^2 k'_3} \left[\frac{e^{-2\pi k'_3/\kappa}}{1 - \cos \theta} \right], \quad (52)$$

under the conditions: $k_3 > k_c$, $k'_3 > k_c$, $\omega' \sim k'_3 \gg \omega$, $\omega \sim k'_3 \gg \kappa$, $\omega \gg \kappa$, and $\theta \neq 0$.

Using (14), (51), and (52), we are able to obtain analytic expressions for their respective particle spectra.

The reflected particle spectrum is

$$\begin{aligned} \frac{dN_{\text{ref}}(0 \leq \theta \leq \pi/2)}{d\omega d\Omega} &\approx \frac{A\omega^2}{4\pi^2} \int_{\Lambda_1}^{\infty} dk'_3 |\beta_{\mathbf{k}\mathbf{k}'}^{\text{ref}}|^2 \\ &= \frac{A\alpha^2}{32\pi^3 \kappa \Lambda_1} \left[1 - \frac{(\omega \sin \theta)^2}{4\Lambda_1^2} \right] \left[\frac{\omega}{e^{\omega/T_{\text{eff}}(\theta)} + 1} \right], \end{aligned} \quad (53)$$

where Λ_1 is a physical infrared cutoff approximated by κ or ω . This cutoff is introduced since (51) is valid for $k'_3 > k_c$ (semi-transparent condition), $k'_3 \gg \omega$, and $k'_3 \gg \kappa$ (the last two conditions make the second term in (43) dominate). Naively, if the parameter κ is less than k_c , then Λ_1 should be approximated by ω since $k'_3 \gg \omega > k_c > \kappa$. However, from (51), we know that α/κ should be less than one since the spectrum should vanish without ambiguity in the no-coupling limit, i.e., $\alpha = 0$. This then rules out the above naive parameter regime since $k_c \sim \alpha$. Therefore, we are only left with the following two legitimate regimes: $k'_3 \gg \kappa > \omega > k_c$ and $k'_3 \gg \omega > \kappa > k_c$. In the former case, Λ_1 should be approximated by κ , whereas, in the latter case, Λ_1 should be approximated by ω instead. Thus, Λ_1 is approximated by κ or ω .

The transmitted particle spectrum is

$$\begin{aligned} \frac{dN_{\text{tran}}(\theta = 0)}{d\omega d\Omega} &\approx \frac{A\omega^2}{4\pi^2} \int_{\Lambda_2}^{\infty} dk'_3 |\beta_{\mathbf{k}\mathbf{k}'}^{\text{tran}}|^2 \\ &\approx \frac{A\alpha^2}{1024\pi^4} \left[\frac{\kappa^2 \omega}{\Lambda_2^4} \right], \\ \frac{dN_{\text{tran}}(0 < \theta \leq \pi/2)}{d\omega d\Omega} &\approx \frac{A\omega^2}{4\pi^2} \int_{\Lambda_2}^{\infty} dk'_3 |\beta_{\mathbf{k}\mathbf{k}'}^{\text{tran}}|^2 \\ &\approx \frac{A\alpha^2}{16\pi^3 \kappa} \left[\frac{\Gamma(0, 2\pi\Lambda_2/\kappa)}{1 - \cos \theta} \right], \end{aligned} \quad (54)$$

where $\Lambda_2 \sim \omega$. This cutoff is introduced since (52) is valid for $k'_3 > k_c$, $k'_3 \gg \omega$, $k'_3 \gg \kappa$, and $\omega \gg \kappa$. There are two possibilities within these regimes, i.e., $k'_3 \gg \omega > \kappa > k_c$ and $k'_3 \gg \omega > k_c > \kappa$. For both situations, Λ_2 should be approximated by ω . However, following similar argument

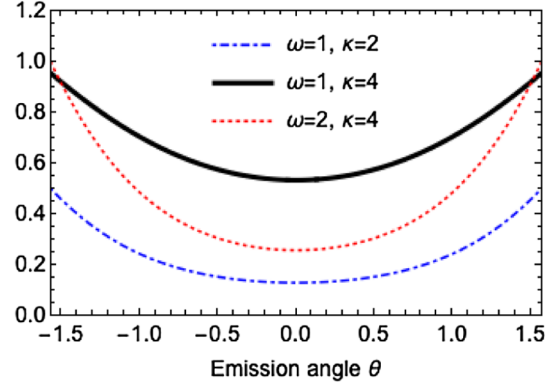


FIG. 1. Angular spectrum for Eq. (53) when $k'_3 \gg \kappa > \omega > k_c$. We roughly take $\Lambda_1 \sim \kappa$ and normalize the spectrum by its value at $\omega = 2$, $\kappa = 4$.

as the case for reflected spectrum, we conclude only the former regime is legitimate.

In (1+3)D spacetime, the number of particles emitted in the off-perpendicular directions due to the reflected modes is larger than those emitted perpendicularly to the mirror's surface, as illustrated in Figs. 1 and 2. In addition, the motion of the mirror being relativistic is also crucial for this phenomenon to occur. This should be expected since, classically, the reflection of photons off a relativistic, receding mirror in 3-dimensional space tends to spread in large angles when the striking process is off-perpendicular [36,37]. Therefore, in our current situation, there are more in-modes reflected off-perpendicularly and thus the excitation of these modes leads to more off-perpendicular particles being created compared to their perpendicular counterparts. As for the particles created by the transmitted modes, they are mainly focused within a small emission angle, as illustrated in Fig. 3. Thus, for a relativistic, plane mirror in (1+3)D, the created perpendicular particles are the product of both the reflected, perpendicular in-modes and the transmitted modes

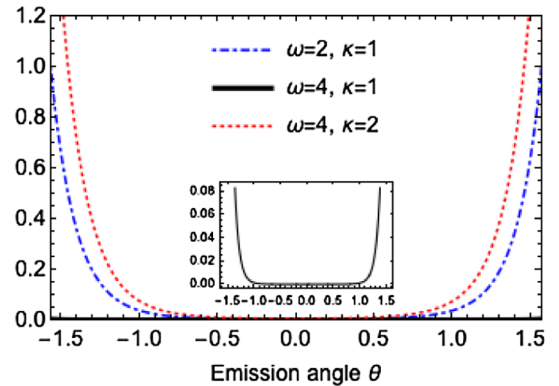


FIG. 2. Angular spectrum for Eq. (53) when $k'_3 \gg \omega > \kappa > k_c$. We take $\Lambda_1 \sim \omega$ and normalize the spectrum by its value at $\omega = 4$, $\kappa = 2$. The subgraph is a zoom-in for the case: $\omega = 4$, $\kappa = 1$ normalized by the value at $\theta = \pi/2$.

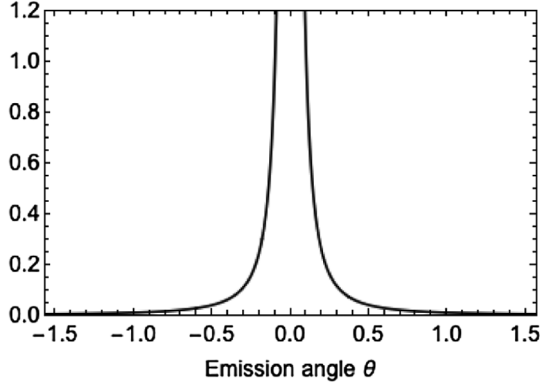


FIG. 3. Angular spectrum for Eq. (54). The spectrum is normalized by the value at $\theta = 0.1$.

although the contribution from the latter may be negligible in comparison. However, for off-perpendicular directions, the created particles may serve as a characteristic product of the reflected in-modes.

Furthermore, the effective temperature $T_{\text{eff}}(\theta)$ is emission angle (θ)-dependent. In the perpendicular direction, i.e., effectively (1 + 1)D, the effective temperature recovers the familiar temperature $T_H \equiv T_{\text{eff}}(\theta = 0) = \kappa/2\pi$ in the (1 + 1)D literature. However, as the emission angle gets larger, the effective temperature monotonically increases and eventually reaches twice the value of $T_{\text{eff}}(\theta = 0) = \kappa/2\pi$ at $\theta = \pi/2$, i.e., $T_{\text{eff}}(\theta = \pi/2) = \kappa/\pi$. This tendency may be understood as a manifestation of the fact that off-perpendicular particles are more probable to be created as mentioned in the last paragraph.

B. Trajectory 2

We now consider one of the trajectories proposed in [22] for a plasma mirror that may be realizable in future experiments. From Eqs. (23) and (28) of [22], one obtains the following trajectory:

$$t_m(z_m) = -\frac{z_m}{\epsilon} + \frac{3\pi}{2\epsilon\omega_{p0}(a+b)} \left[\frac{a+b}{a+be^{z_m/D}} - 1 \right], \quad (55)$$

where $\{\omega_{p0}, a, b, D\} > 0$ are positive constants, $-\infty < z_m \leq 0$, $0 \leq t_m < \infty$, $0 < \epsilon \leq 1$, and we have made the mirror left-moving as opposed to the original right-moving setup in [22]. For simplicity, we will take $\epsilon = 1$ and $a = 1$ hereafter. This trajectory is designed such that it asymptotes the Davies-Fulling trajectory [4], which mimics gravitational collapse by a point mirror in (1 + 1)D, in the late time $t_m \rightarrow \infty$ or simply in the limit: $a \gg b$. Therefore, one would expect to obtain similar particle spectra for this trajectory as the previous example. The above trajectory only describes the accelerating phase of the mirror. Before the mirror accelerates, i.e., $-\infty < t_m \leq 0$, it moves at a constant velocity approaching the speed of light [22]:

$$t_m(z_m) = -\frac{z_m}{v}, \quad 0 \leq z_m < \infty, \quad v \rightarrow 1. \quad (56)$$

Having the trajectories, we now compute the corresponding beta-coefficient on the mirror's right due to the reflected modes.

$$\begin{aligned} \beta_{\mathbf{k}\mathbf{k}'}^{\text{ref}}(k'_3 > 0) &\approx \frac{\alpha}{4\pi i \sqrt{\omega\omega'}} \int_{-\infty}^{\infty} dt_m \gamma^{-1}(t_m) e^{i(\omega+\omega')t_m - i(k_3 - k'_3)z_m(t_m)} \\ &= \frac{\alpha}{4\pi i \sqrt{\omega\omega'}} \int_{-\infty}^{\infty} dz_m \frac{t'_m \sqrt{t_m'^2 - 1}}{|t'_m|} e^{i(\omega+\omega')t_m - i(k_3 - k'_3)z_m(t_m)} \\ &\approx -\frac{\alpha}{4\pi \sqrt{\omega\omega'}} \left[\frac{\sqrt{1-v^2}}{\omega^+ + vk_3^-} \right] \\ &\quad + \frac{\alpha e^{\frac{3i\pi\omega^+ b}{2\omega_{p0}}} \sqrt{3\pi b}}{4\pi i \sqrt{\omega\omega'} \omega_{p0} D} \int_0^{\infty} dz_m e^{-\frac{iz_m}{2D}} e^{i(\omega^+ + k_3^-)z_m} e^{-\frac{3i\pi\omega^+ b}{2\omega_{p0}} e^{-\frac{z_m}{D}}}, \end{aligned}$$

where $\omega = |\mathbf{k}|$, $\omega' = |\mathbf{k}'|$, $t'_m = dt_m/dz_m$, $\omega^+ = \omega + \omega'$, $k_3^- = k_3 - k'_3$, and the second “ \approx ” refers to assuming $b \ll \omega_{p0}D$ (this makes the velocity more continuous at $t_m = 0$), $b \ll 1$ (this makes the trajectory Davies-Fulling-like), $\omega^+ \ll \omega_{p0}b^{-2}$ and leaving terms to the leading order. The integral in the last line can be done by performing contour integrations in the complex plane. The result is

$$\begin{aligned} \beta_{\mathbf{k}\mathbf{k}'}^{\text{ref}}(k'_3 > 0) &\approx -\frac{\alpha}{4\pi \sqrt{\omega\omega'}} \left[\frac{\sqrt{1-v^2}}{\omega^+ + vk_3^-} \right] \\ &\quad - \frac{\alpha \sqrt{2D} e^{\frac{3i\pi\omega^+ b}{2\omega_{p0}}} e^{\frac{i\pi}{4}} e^{-\frac{\pi D(\omega^+ + k_3^-)}{2}}}{4\pi \sqrt{\omega^+} \sqrt{\omega\omega'}} \\ &\quad \times \left[\frac{3\pi\omega^+ b}{2\omega_{p0}} \right]^{iD(\omega^+ + k_3^-)} \left\{ \Gamma \left[\frac{1}{2} - iD(\omega^+ + k_3^-) \right] \right. \\ &\quad \left. - \Gamma \left[\frac{1}{2} - iD(\omega^+ + k_3^-), \frac{3i\pi\omega^+ b}{2\omega_{p0}} \right] \right\}. \quad (57) \end{aligned}$$

By further taking the limit: $\omega^+ b \gg \omega_{p0}$ and recalling $v \rightarrow 1$, (57) simplifies to

$$\begin{aligned} \beta_{\mathbf{k}\mathbf{k}'}^{\text{ref}}(k'_3 > 0) &\approx \frac{\alpha}{4\pi\omega^+ \sqrt{\omega\omega'}} \sqrt{\frac{4D\omega_{p0}}{3\pi b}} \\ &\quad - \frac{\alpha \sqrt{2D} e^{\frac{3i\pi\omega^+ b}{2\omega_{p0}}} e^{\frac{i\pi}{4}} e^{-\frac{\pi D(\omega^+ + k_3^-)}{2}}}{4\pi \sqrt{\omega^+} \sqrt{\omega\omega'}} \\ &\quad \times \left[\frac{3\pi\omega^+ b}{2\omega_{p0}} \right]^{iD(\omega^+ + k_3^-)} \Gamma \left[\frac{1}{2} - iD(\omega^+ + k_3^-) \right]. \quad (58) \end{aligned}$$

Its modulus squared is

$$|\beta_{\mathbf{k}\mathbf{k}'}^{\text{ref}}(k'_3 > 0)|^2 \approx \frac{\alpha^2 D}{4\pi\omega\omega'\omega^+} \left[\frac{1}{e^{2\pi D(\omega^+ + k'_3)} + 1} \right] + \text{terms irrelevant to our interest.} \quad (59)$$

For $\omega' \sim k'_3$, (59) becomes

$$|\beta_{\mathbf{k}\mathbf{k}'}^{\text{ref}}(k'_3 > 0)|^2 \approx \frac{\alpha^2 D}{4\pi\omega k'_3(\omega + k'_3)} \left[\frac{1}{e^{\omega/T_{\text{eff}}(\theta)} + 1} \right] + \text{terms irrelevant to our interest,} \quad (60)$$

where $T_{\text{eff}}(\theta) = 1/[(1 + \cos\theta)2\pi D]$ is identified as an effective temperature. For particles emitted perpendicularly to the mirror's surface, i.e., $\theta = 0$, the temperature becomes $T_H \equiv T_{\text{eff}}(\theta = 0) = 1/4\pi D$, which leads to the identification of the surface gravity of an analog black hole as $\kappa = 1/2D$. For $\omega' \sim k'_3 \gg \omega$ (late time), the corresponding particle spectrum is

$$\begin{aligned} \frac{dN_{\text{ref}}(0 \leq \theta \leq \pi/2)}{d\omega d\Omega} &\approx \frac{A\omega^2}{4\pi^2} \int_{\Lambda_1}^{\Lambda_2} dk'_3 |\beta_{\mathbf{k}\mathbf{k}'}^{\text{ref}}|^2 \\ &= \frac{A\alpha^2}{32\pi^3 \kappa} \left[\frac{1}{\Lambda_1} - \frac{1}{\Lambda_2} \right] \left[\frac{\omega}{e^{\omega/T_{\text{eff}}(\theta)} + 1} \right] \\ &+ \text{terms irrelevant to our interest,} \quad (61) \end{aligned}$$

where $\Lambda_1 \sim \omega \vee \omega_{p0} b^{-1}$ and $\Lambda_2 \sim \omega_{p0} b^{-2}$. Since (61) is derived under several above-mentioned assumptions, the only possible legitimate cases are: (i) $\omega_{p0} b^{-2} \gg k'_3 \gg \omega > k_c > \omega_{p0} b^{-1}$, (ii) $\omega_{p0} b^{-2} \gg k'_3 \gg \omega > \omega_{p0} b^{-1} > k_c$, and (iii) $\omega_{p0} b^{-2} \gg k'_3 \gg \omega_{p0} b^{-1} > \omega > k_c$, for (61) to be valid. For (i) and (ii), the infrared cutoffs are both approximately ω , whereas the infrared cutoff for (iii) is approximately $\omega_{p0} b^{-1}$. However, for all cases, the upper cutoffs are approximately $\omega_{p0} b^{-2}$, which originates from the condition $\omega^+ \ll \omega_{p0} b^{-2}$ imposed at the very beginning. Notice that the condition: $k_c \sim \alpha < \kappa = 1/2D$ is also obeyed by the above spectra based on similar argument addressed in the previous subsection. However, in the current example, this condition is irrelevant to the determination of legitimate parameter regimes.

The spectra for this trajectory contain the same distributions, which are the parts relevant to mimic gravitational collapse, as (51) and (53). The spectra also contain two terms, which are contributed from the first term in (58) and its cross-term with the Gamma function term, that are not relevant to our interest of mimicking gravitational collapse. Nevertheless, by comparing the modulus squared of the first term in (58) to the second term involving the Gamma function, we find the first terms in (60) and (61) dominate over the terms irrelevant to our interest in the regime: $\omega \ll \kappa \ln[bk'_3/\omega_{p0}]$.

Consider future flying plasma mirror experiments [22,38] with $n_s = 1.6 \times 10^5$ (eV)², $\alpha = 2.8 \times 10^{-2}$ eV,

$\omega_{p0} = 0.6 \times 10^{-2}$ eV, and $D = 0.5 \mu\text{m}$, the corresponding characteristic frequency of the emitted particle would be $\omega_{\text{char}} = T_{\text{eff}} \sim 1/4\pi D = 3.1 \times 10^{-2}$ eV $> \omega_{p0}$, i.e., these emitted particles can propagate through the plasma for detection. In addition, for, say, $b = 0.2$, condition (ii) is satisfied and the emitted particles within the frequency range: $3. \times 10^{-2}$ eV $< \omega < 14.8 \times 10^{-2}$ eV should distribute themselves according to (61).

In this subsection, we omit the computation of quantities due to the transmitted modes since we are only interested in quantities that can be associated with an analog black hole. However, these computations should follow straightforwardly as the discussions made in the previous example.

V. CONCLUSION

In this paper, we have investigated the production of massless, scalar particles by a relativistic, semi-transparent, plane mirror with arbitrary, relativistic trajectories based on the Barton-Calogeracos (BC) action and derived the corresponding particle spectrum in (1+3)D Minkowski spacetime and identified the relation between the spectrum and the particle production probability. Comparisons of our treatment to the approaches adopted in the (1+1)D literature for a relativistic, point mirror and the (1+3)D literature for a nonrelativistic, plane mirror are summarized in Tables I and II.

We apply our derived (1+3)D spectrum formula to the trajectory that is often used in the (1+1)D literature to mimic gravitational collapse. The spectra in various frequency/momentum regimes are derived analytically. In particular, in the regime $\omega' \gg \omega$ and $\omega' \gg \kappa$, we find the particle spectrum created by the reflected in-modes has an effective temperature depending on the emission angle monotonically and the conventional (1+1)D result is recovered at $\theta = 0$. In addition, there are more particles created with nonvanishing transverse momenta compared to the perpendicular ones due to the relativistic property of the mirror and the spacetime dimension being (1+3)D.

As a second example, we apply our derived spectrum formula to the Chen-Mourou trajectory proposed in [22]. This trajectory asymptotes the Davies-Fulling trajectory [4] in the limits: $t_m \rightarrow \infty$ or $a \gg b$. Thus, there will be a period which mimics gravitational collapse for a (1+1)D moving mirror model. For the sake of analytic computations to extract the explicit distribution of the particle spectrum, we make some assumptions throughout the discussion and find the corresponding particle spectrum due to the reflected modes is similar to that of the previous example, which should be expected, and thus the discussions made previously also apply directly to this case.

In this paper, the mirror considered is an infinite-size, homogeneous, plane mirror in (1+3)D Minkowski spacetime. However, the formalism adopted in principle allows the consideration of a mirror with finite size by, e.g.,

inserting a density function describing the mirror's transverse geometry. In addition, the geometric factor of the mirror is incorporated into the particle spectra, i.e., (53) and (54), via the area A , which has a dimension of length². If we group a factor of ω^2 to the area A , they combine to give $A/\lambda^2 \rightarrow \infty$, where λ is the wavelength of the particle (another ω^2 should be divided by α^2 simultaneously giving the semitransparent condition $\alpha/\omega \ll 1$). This observation indicates that the quantities we discussed are valid in the realm of geometric optics. When the finite-size effect is considered, the characteristic length \sqrt{A} may be comparable to the wavelength λ . In such a case, diffraction may occur and the particle spectrum may include other corrections in terms of the characteristic length. The issue of finite-size effect will be further investigated in our upcoming work.

ACKNOWLEDGMENTS

The authors appreciate helpful discussions with Yung-Kun Liu of National Taiwan University. This work is supported by ROC Ministry of Science and Technology (MOST), National Center for Theoretical Sciences (NCTS), and Leung Center for Cosmology and Particle Astrophysics (LeCosPA) of National Taiwan University. P. C. is in addition supported by U.S. Department of Energy under Contract No. DE-AC03-76SF00515.

APPENDIX: S-MATRIX APPROACH

In this Appendix, we offer an alternative and fast way for computing the particle spectrum. This approach begins by recognizing the S-matrix of the BC action as

$$\mathbb{S} = \mathcal{T} e^{-\frac{i\alpha}{2} \int_{\mathbb{R}} d^4x \gamma^{-1}(x_0) \delta(x_3 - q(x_0)) \hat{\phi}_I^2(x)}, \quad (\text{A1})$$

where \mathcal{T} is the time-ordering operator and the subscript I refers to the interaction picture.

By using the relation between the in-state/operator and the out-state/operator:

$$|0, \text{out}\rangle = \mathbb{S}|0, \text{in}\rangle \quad \text{and} \quad \hat{a}_{\mathbf{k}}^{\text{out}} = \mathbb{S}^\dagger \hat{a}_{\mathbf{k}}^{\text{in}} \mathbb{S}, \quad (\text{A2})$$

and the identity (for later convenience):

$$\begin{aligned} & \langle 0, \text{in} | \hat{a}_{\mathbf{k}'}^{\text{in}} \hat{a}_{\mathbf{p}}^{\text{in}} \hat{a}_{\mathbf{k}}^{\text{in}\dagger} \hat{a}_{\mathbf{k}}^{\text{in}} \hat{a}_{\mathbf{p}'}^{\text{in}\dagger} \hat{a}_{\mathbf{q}}^{\text{in}\dagger} | 0, \text{in} \rangle \\ &= \delta(\mathbf{k}' - \mathbf{q}) \delta(\mathbf{p} - \mathbf{k}) \delta(\mathbf{k} - \mathbf{p}') + \delta(\mathbf{k}' - \mathbf{k}) \delta(\mathbf{k} - \mathbf{p}') \delta(\mathbf{p} - \mathbf{q}) \\ & \quad + \delta(\mathbf{k}' - \mathbf{p}') \delta(\mathbf{p} - \mathbf{k}) \delta(\mathbf{q} - \mathbf{k}) \\ & \quad + \delta(\mathbf{k}' - \mathbf{k}) \delta(\mathbf{q} - \mathbf{k}) \delta(\mathbf{p} - \mathbf{p}'), \end{aligned} \quad (\text{A3})$$

we may then compute the particle spectrum by

$$\begin{aligned} \frac{dN}{d^2k_\perp dk_3} &= \langle 0, \text{in} | \hat{a}_{\mathbf{k}}^{\text{out}\dagger} \hat{a}_{\mathbf{k}}^{\text{out}} | 0, \text{in} \rangle \\ &= \langle 0, \text{in} | \mathbb{S}^\dagger \hat{a}_{\mathbf{k}}^{\text{in}\dagger} \hat{a}_{\mathbf{k}}^{\text{in}} \mathbb{S} | 0, \text{in} \rangle \\ &\approx \frac{A\alpha^2}{64\pi^4 |\mathbf{k}|} \int_{\mathbb{D}} dk'_3 \frac{1}{\sqrt{k_\perp^2 + k_3'^2}} \\ & \quad \times \left| \int_{\mathbb{R}} dx'_0 \gamma^{-1}(x'_0) e^{i(|\mathbf{k}| + \sqrt{k_\perp^2 + k_3'^2})x'_0 - i(k_3 + k'_3)q(x'_0)} \right|^2, \end{aligned} \quad (\text{A4})$$

which agrees exactly with our previous result, Eq. (14). The advantage of the S-matrix approach is that it enables one to obtain the particle spectrum directly in a simpler manner without the need of finding the mode functions, Eqs. (6) and (8), first and performing laborious calculations. Nevertheless, the mode functions derived in the main text may be important for future studies of, e.g., energy-momentum tensor, correlation functions, detector response function, etc.

-
- [1] G. T. Moore, *J. Math. Phys. (N.Y.)* **11**, 2679 (1970).
 - [2] B. S. DeWitt, *Phys. Rep.* **19**, 295 (1975).
 - [3] S. A. Fulling and P. C. W. Davies, *Proc. R. Soc. A* **348**, 393 (1976).
 - [4] P. C. W. Davies and S. A. Fulling, *Proc. R. Soc. A* **356**, 237 (1977).
 - [5] M. R. R. Good, Ph.D. thesis, University of North Carolina at Chapel Hill, 2011.
 - [6] M. R. R. Good, P. R. Anderson, and C. R. Evans, *Phys. Rev. D* **88**, 025023 (2013).
 - [7] P. Chen and D. H. Yeom, *Phys. Rev. D* **96**, 025016 (2017).
 - [8] P. A. M. Neto and L. A. S. Machado, *Phys. Rev. A* **54**, 3420 (1996).
 - [9] P. A. M. Neto and L. A. S. Machado, *Braz. J. Phys.* **25**, 324 (1995), <https://www.semanticscholar.org/paper/Radiation-Force-for-a-Mirror-in-Vacuum-P-Ma%3%ADa/3e44e29328abeb7778fdbac424bd28b365df0437?p2df>.
 - [10] M. F. Maghrebi, R. Golestanian, and M. Kardar, *Phys. Rev. D* **87**, 025016 (2013).
 - [11] A. L. C. Rego, B. W. Mintz, C. Farina, and D. T. Alves, *Phys. Rev. D* **87**, 045024 (2013).
 - [12] J. D. L. Silva, A. N. Braga, A. L. C. Rego, and D. T. Alves, *Phys. Rev. D* **92**, 025040 (2015).
 - [13] L. H. Ford and A. Vilenkin, *Phys. Rev. D* **25**, 2569 (1982).
 - [14] W. R. Walker, *Phys. Rev. D* **31**, 767 (1985).

- [15] P. Candelas and D. J. Raine, *J. Math. Phys. (N.Y.)* **17**, 2101 (1976).
- [16] P. Candelas and D. Deutsch, *Proc. R. Soc. A* **354**, 79 (1977).
- [17] W. G. Anderson and W. Israel, *Phys. Rev. D* **60**, 084003 (1999).
- [18] L. Hadasz, M. Sadzikowski, and P. Wegrzyn, [arXiv:hep-th/9803032](https://arxiv.org/abs/hep-th/9803032).
- [19] V. P. Frolov and E. M. Serebriany, *J. Phys. A* **12**, 2415 (1979).
- [20] C. M. Wilson, G. Johansson, A. Pourkabirian, M. Simoen, J. R. Johansson, T. Duty, F. Nori, and P. Delsing, *Nature (London)* **479**, 376 (2011).
- [21] P. Chen and G. Mourou, *Phys. Rev. Lett.* **118**, 045001 (2017).
- [22] P. Chen and G. Mourou, [arXiv:2004.10615](https://arxiv.org/abs/2004.10615).
- [23] G. Barton and A. Calogeracos, *Ann. Phys. (N.Y.)* **238**, 227 (1995).
- [24] C. R. Galley, R. O. Behunin, and B. L. Hu, *Phys. Rev. A* **87**, 043832 (2013).
- [25] J. Haro and E. Elizalde, *Phys. Rev. D* **77**, 045011 (2008).
- [26] J. Haro, [arXiv:1011.4772v2](https://arxiv.org/abs/1011.4772v2).
- [27] E. Elizalde and J. Haro, *Phys. Rev. D* **81**, 128701 (2010).
- [28] N. Nicolaevici, *Phys. Rev. D* **80**, 125003 (2009).
- [29] N. Nicolaevici, *Classical Quantum Gravity* **18**, 619 (2001).
- [30] J. Haro and E. Elizalde, *Phys. Rev. Lett.* **97**, 130401 (2006).
- [31] A. Calogeracos, *J. Phys. A* **35**, 3415 (2002).
- [32] C. D. Fosco, A. Giraldo, and F. D. Mazzitelli, *Phys. Rev. D* **96**, 045004 (2017).
- [33] This is an integral equation that can be solved iteratively.
- [34] Unitarity guarantees that $|R|^2 + |T|^2 = 1$. However, some caution is required when one computes quantities such as $|R|^2 + |T|^2 = 1$ and $R + T = 1$ in the expansion of α . For example, to verify $|R|^2 + |T|^2 = 1$ to the accuracy of second order in α , it is sufficient to retain up to the first order in R , whereas one must keep track to the second order in T . This is because the interference between the zeroth order and the second order of T also contributes to $|T|^2$. In contrast, to check $R + T = 1$, both R and T can be expanded to the same order since there is no interference involved.
- [35] During acceleration, the reflection coefficient may be manipulated as, e.g., $R^R(v) \sim \frac{\alpha}{2} \int_{\tau}^{\tau_A} d\tau' e^{\alpha(\tau-\tau')/2}(\dots) = \frac{\alpha(\tau_A-\tau)}{2} \int_0^1 d\sigma e^{-\alpha(\tau_A-\tau)\sigma/2}(\dots)$, where we have made a change of variable by $\tau' - \tau = (\tau_A - \tau)\sigma$. This also demonstrates that the first-order approximation corresponds to the semi-transparent limit, i.e., $|R^R| \ll 1$. For more discussion on this, please see [27,28].
- [36] A. Einstein, *Ann. Phys. (Berlin)* **322**, 891 (1905).
- [37] A. Gjurchinovski and A. Skeparovski, *Phys. Teacher* **46**, 416 (2008).
- [38] C. E. Chou, K. N. Lin, and P. Chen (to be published).